

INFLUENCE OF QUENCHING/PARTITIONING TEMPERATURE ON MORPHOLOGY OF 37MnSi5 STEEL

H. R. GHAZVINLOO, A. HONARBAKHSH-RAOUF

Department of Materials Engineering, Semnan University, Semnan, Iran

In the last two decades an extreme tendency towards the development of the third-generation of advanced high-strength steels for the automotive industry can be observed. As a novel heat treatment process quenching and partitioning was originally proposed by Speer et al. This process is one of the new strategies to produce the steel with a combination of high strength and considerable ductility. The influence of quenching/partitioning temperature on morphology and microstructure of 37MnSi5 steel during quenching and partitioning process was studied. To this aim, 210, 238 and 270°C were chosen as quenching temperature, and 300, 400 and 450°C as partitioning temperature. After the heat treatments the microstructural characteristics were evaluated, compared, and discussed using a scanning electron microscope and a field emission-scanning electron microscope.

Keywords: *quenching/partitioning temperature, microstructure, 37MnSi5 steel.*

The past few decades have witnessed a significant research effort directed towards the development of advanced high-strength steel (AHSS) grades for automotive applications, as they provide an opportunity for the development of cost-effective and light-weight parts with improved safety and optimized environmental performance [1–3]. The quenching and partitioning (Q&P) proposed by Speer et al. [4, 5] is receiving increased attention as a novel heat treatment to produce AHSS that contain martensite/retained austenite mixtures in microstructure. The Q&P steel shows a good combination of strength-ductility in which martensite acts as a strengthening phase and retained austenite contributes significantly to the ductility. The Q&P process usually consists of a two-step heat treatment. First, the steel is held at a temperature in the full austenite (γ) or intercritical ($\gamma+\alpha$) range and then quenched to a temperature between the martensite-start (M_s) temperature and martensite-finish (M_f) temperature. Second, the quenched steel is held either at, or above, the initial quenching temperature in order to enrich the untransformed austenite by carbon diffusion from supersaturated martensite [6, 7]. The increased carbon in the austenite decreases its M_s temperature so that thermally stable austenite is obtained after the final quenching to room temperature. The Q&P process is mainly applied to steels with chemical compositions similar to those of conventional transformation-induced plasticity (TRIP) steels [8, 9]. Significant additions of elements such as silicon retard the formation of carbides and give rise to the carbon enrichment of austenite via partitioning of carbon from supersaturated martensite [8, 10]. Manganese, nickel, and chromium are included in the chemical composition to retard ferrite, pearlite and bainite formation and to decrease the bainite start temperature, as well as to enhance the austenite stability [11]. It has been suggested that the carbon partitioning from martensite into austenite is controlled by the constrained carbon equilibrium (CCE) criterion [4]. This criterion aims to predict the carbon concentration in austenite under the condition where: competing reactions, such as cementite or transition carbide formation or bainite transformation are suppressed; an identical carbon chemical potential

exists in both ferrite (or martensite) and austenite; the carbon partitioning proceeds under the assumption that the interface between ferrite and austenite does not migrate [12]. There is still a lack of information on the exact microstructural characterization of steels after Q&P treatment [13]. A more accurate description of the microstructure is essential for better understanding of the microstructure formation and better control of the final properties of the material [13]. Experimental investigations of microstructural processes during Q&P can enhance our understanding of the Q&P process, and may be important for adjusting and tailoring the required mechanical properties of Q&P steels [14]. In this study the effect of quenching/partitioning temperature on morphological and microstructural evolutions of 37MnSi5 steel during the Q&P process is investigated.

Experimental procedure. The studied alloy in this work was low-alloy 37MnSi5 steel with a composition similar to conventional TRIP-assisted steels (wt.%): C – 0.362; Si – 1.38; Mn – 1.24; Cr – 0.0973; Ni – 0.0902; Cu – 0.0711; Al – 0.03; Pb – 0.025; P – 0.0245; S – 0.0202; W – 0.015; Co – 0.0101; As – 0.0101; Sn – 0.0095; Mo – 0.005; Nb – 0.0025; Ti – 0.0023; B – 0.002; Zr – 0.002; V – 0.002.

$M_s = 338.73^\circ\text{C}$ for this alloy and is determined from Eq. (1) [15]:

$$M_s (^\circ\text{C}) = 539 - 423C - 30.4\text{Mn} - 7.5\text{Si} + 30\text{Al}, \quad (1)$$

where C, Mn, Si, and Al are the elemental contents (wt.%). The critical temperatures of Ac_1 and Ac_3 for base material were estimated using dilatometric test. A cylindrical specimen with a diameter of 5 mm and a height of 20 mm was used as dilatometric specimen in a LINSEIS type dilatometer. The $Ac_1 = 748.1^\circ\text{C}$ and $Ac_3 = 841.5^\circ\text{C}$, are measured by this method.

For Q&P heat treatments, samples (15 mm×10 mm×3 mm) were fully austenitized at 900°C for 10 min in a furnace (model K20L1200), quenched in an oil bath at 210; 238, and 270°C with a cooling rate of -220°C/s , then partitioned at these temperatures for 100 s and water-quenched to room temperature in one-step Q&P heat treatment; held for 10 s, partitioned at temperatures of 300, 400 and 450°C in a bath of molten salt for 100 s, and water-quenched to room temperature in two-step Q&P heat treatment. Schematic diagram of the one and two-step Q&P applied is shown in Fig. 1.

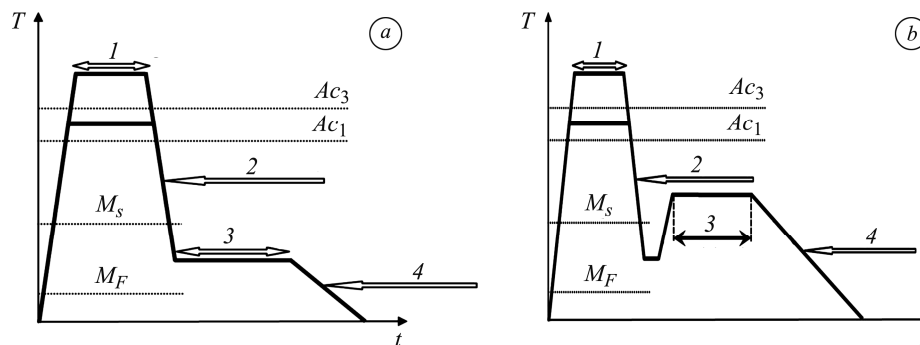


Fig. 1. Scheme of the one-step (a) and two-step (b) Q&P applied in this study: 1 – austenitizing; 2, 4 – initial and final quenching; 3 – partitioning.

After the Q&P heat treatments, the treated specimens were ground and polished mechanically with alumina and then etched with 2% Nital (nitric acid in ethanol) for 6...8 s. Microstructural examinations for the treated specimens were conducted using a JEOL (JXA-840, operating at 15 and 25 kV) scanning electron microscope (SEM) and a HITACHI (S-4160, operating at 30 kV) field emission-scanning electron microscope (FE-SEM).

In order to determine the volume fraction of retained austenite and its average carbon content in the treated specimens, X-ray diffraction (XRD) measurements were performed on a Bruker D8 diffractometer using a $\text{CuK}\alpha$ radiation operating at 35 kV

and 30 mA. Specimens were scanned over a 2θ -range of $10^\circ \dots 90^\circ$ with a dwell time of 1 s and a step size of 0.05° . The volume fraction of retained austenite was measured based on the direct comparison method [16] from the integrated intensity of the $(200)_\gamma$, $(220)_\gamma$, $(200)_M$, and $(211)_M$ peaks, and the average carbon content of retained austenite was calculated using Eq. (2) [17]. The average carbon content obtained from both austenite peak positions was calculated [18] in this study.

$$a_0 = 3.555 + 0.044 x, \quad (2)$$

where a_0 – the austenite lattice parameter in angstroms; x – average carbon content of austenite in weight percent.

The experimental results. SEM microscopy observations. SEM micrographs of the specimens heat treated at different quenching temperatures are shown in Fig. 2. This figure shows the introduction of carbon-enriched retained austenite phase into the martensitic matrix structure. The martensite with lath-type morphology is surrounded by retained austenite and the general feature of the lath-like martensite configuration does not change at different quenching temperatures. The retained austenite with two types of morphological structures is visible in microstructure. One has an island-like shape and is distributed mainly along the grain boundary, and a few are distributed within the martensite matrix. The other has a film-like shape and is distributed between martensite laths [19]. The austenitic films with somewhat higher thickness and elongation and varied orientations are observed in the microstructure of specimen heat treated at optimum quenching temperature in one-step Q&P. On the other hand, the austenitic films with greater thickness along with many austenitic islands, that were larger than a micrometer, can be seen in the microstructure of specimen heat treated at optimum quenching temperature in two-step Q&P. For the specimen heat treated at a quenching temperature of 270°C , more retained austenite was as island-like in one-step Q&P, and as film-like between martensite laths in two-step Q&P.

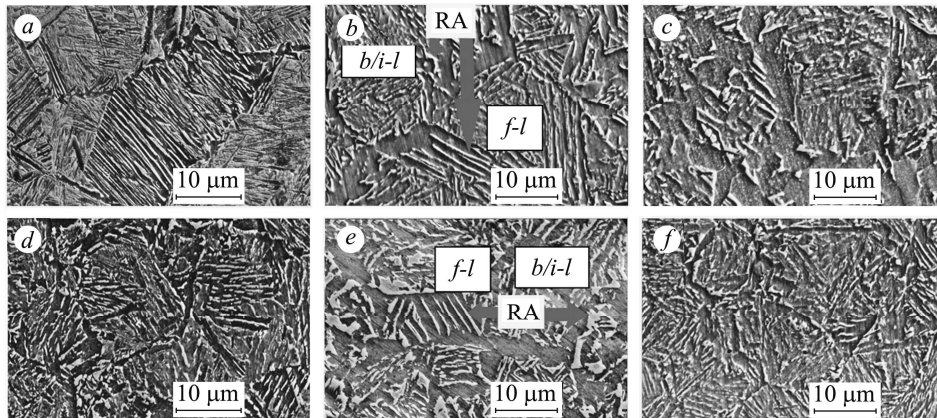


Fig. 2. SEM micrographs of specimen quenched to 210°C (a), 238°C (b) and 270°C (c), partitioned at the same temperatures (one-step); quenched to 210°C (d), 238°C (e) and 270°C (f), partitioned at 400°C (two-step) (RA: retained austenite, *f-l*: film-like, and *b/i-l*: blocky/island-like).

SEM micrographs of the specimens heat treated at different partitioning temperatures are shown in Fig. 3. Similarly, lath-type morphology for martensite and film/island-types for retained austenite are observed in these conditions. Cementite-carbide (Fe_3C) precipitations within the initial martensite laths were characterized in a sample partitioned at 450°C for 100 s, and the dominant shape was quasispherical with a submicron size whereas, no carbide was observed for partitioning temperatures of 300°C and 400°C for the same time. The higher partitioning temperature accelerates the kine-

tics of competitive interactions like tempering of initial martensite and as a result, it provides a considerable potential for precipitating the iron-carbide in initial martensite at a shorter partitioning time. The microstructure of the cementite-carbide in the specimen quenched to 238°C and partitioned at 450°C for 100 s was further examined in higher magnification by a FE-SEM micrograph (Fig. 3).

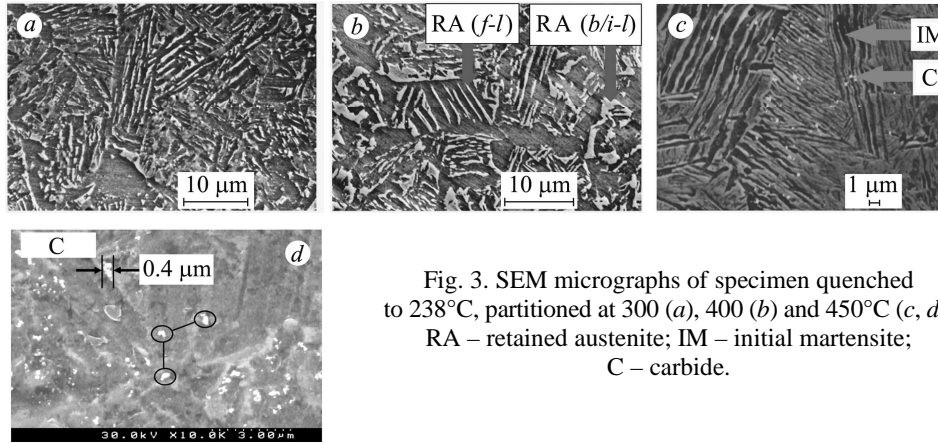


Fig. 3. SEM micrographs of specimen quenched to 238°C, partitioned at 300 (a), 400 (b) and 450°C (c, d): RA – retained austenite; IM – initial martensite; C – carbide.

The presence of carbides is of importance because it implies that the cementite may not have fully dissolved and the available carbon content does not fully contribute to the stabilization of the austenite in the industrial processing conditions employed [20]. Bainitic transformation was not observed for partitioning temperatures of 400 and 450°C in this study and this may be due to the relatively short partitioning time applied in this study (100 s).

XRD results. The average carbon content of the retained austenite obtained for different quenching temperatures is shown in Fig. 4. As shown in this Figure, the highest values of carbon content in one and two-step Q&P were 1.4022% and 1.3068%, respectively which were obtained in optimum quenching temperature (238°C).

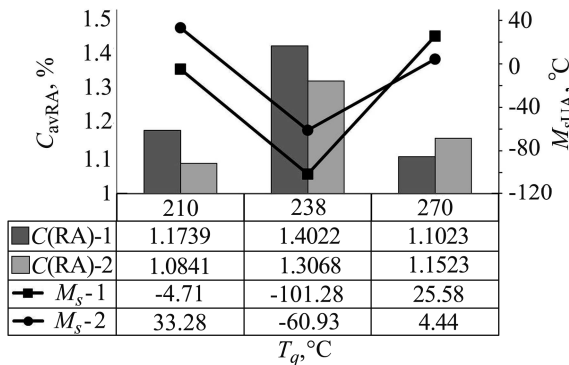


Fig. 4. Average carbon content of retained austenite and M_s temperature of untransformed austenite for specimen quenched to 210, 238 and 270°C, partitioned at the same temperatures (-1); partitioned at 400°C (-2).

A quenching temperature determines the fraction of martensite that is supposed to provide carbon for partitioning to the adjacent austenite during the isothermal holding following quenching [21]. An optimum quench temperature is where just the right amount of martensite is formed during the initial quench to carbon-enrich the untransformed austenite after full partitioning to reduce its M_s temperature to room temperature [22], and yields a maximum amount of retained austenite at the end of the process. At quench temperatures above this optimum quench temperature, substantial untransformed austenite remains after the initial quench but the carbon escaping from the lower volume of martensite is insufficient to stabilize austenite such that fresh martensite is formed during quenching to room temperature. Below the optimum quench

temperature too much austenite is transformed by the initial quench (although sufficient carbon is available for its complete stabilization) [22]. The negligible fractions of untransformed austenite cannot be receptive to a lot of carbon atoms, thus the carbon content of austenite is not considerable in this condition. Overall, an optimum quenching temperature in Q&P process ensure a maximum carbon content for austenite that minimizes its M_s temperature, and so maximizes its thermal stability. The optimum quenching temperature of 238°C in this study could reduce the M_s temperature of austenite to -101.28°C and -60.93°C in one-step and two-step Q&P, respectively. The average carbon content of retained austenite for quenching temperatures of 210°C and 238°C was greater in one-step Q&P compared to two-step Q&P (0.0898%, 0.0954%), whereas two-step Q&P could provide the more carbon content (0.05%) for retained austenite at a quenching temperature of 270°C.

The average carbon content of the retained austenite for different partitioning temperatures is shown in Fig. 5. With an increase in partitioning temperature from 300 to 450°C, activation energy for diffusion of the carbon atoms from supersaturated martensite to adjacent austenite increases (see Fig. 5). In other words, the higher partitioning temperature accelerates kinetics of carbon partitioning, increases the carbon content of retained austenite from 1.3545 to 1.4023%, and reduces its M_s temperature to ~20°C. Carbide precipitation decreases an average carbon content of retained austenite because carbide formation consumes certain amount of carbon in martensite, therefore there may not be enough carbon for the stabilization of untransformed austenite during cooling from partitioning temperature to room temperature [23]. Despite all these, apparently the kinetics of carbon partitioning has been a dominant factor especially at 450°C, and this has led to increase in the average carbon content of retained austenite to 1.4023%.

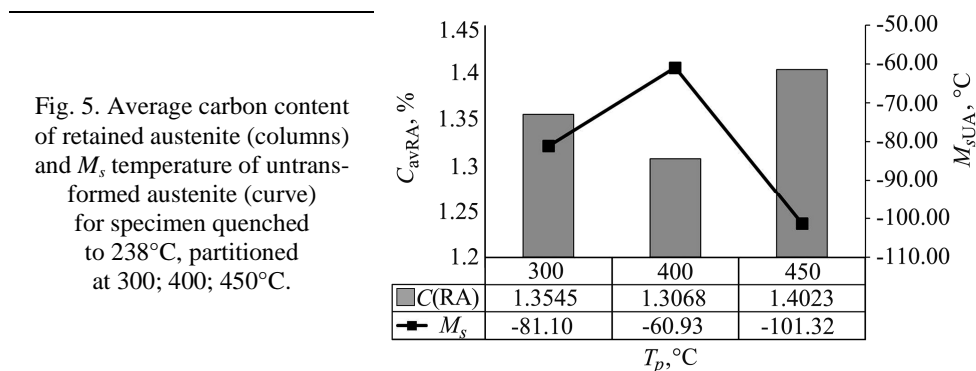


Fig. 5. Average carbon content of retained austenite (columns) and M_s temperature of untransformed austenite (curve) for specimen quenched to 238°C, partitioned at 300; 400; 450°C.

The volume fractions of retained austenite for different quenching and partitioning temperatures are shown in Fig. 6. The optimum quenching temperature could yield a maximum amount of retained austenite (10.85% and 13.58%) in end of one and two-step Q&P.

For all quenching temperatures in this study the volume fraction of retained austenite was larger in two-step Q&P compared to one-step Q&P, and the differences for quenching temperature of 210, 238, and 270°C were 3.08, 2.73, and 0.3%, respectively. The difference in volume fractions of retained austenite decreased in higher quenching temperatures. With increase in quench temperature from 210 to 270°C, the volume fraction of retained austenite first increased and arrived at a maximum at optimum quenching temperature (238°C), and then decreased.

The volume fraction of retained austenite increased from 10.14 to 11.43% with increase in partitioning temperature from 300 to 450°C and it was because of the increase in carbon content of untransformed austenite from 1.3545 to 1.4023%. This result is similar to previous research [18] on 0.17C-1.65Mn-0.38Si-1.11Al-0.08P (wt.%) steel.

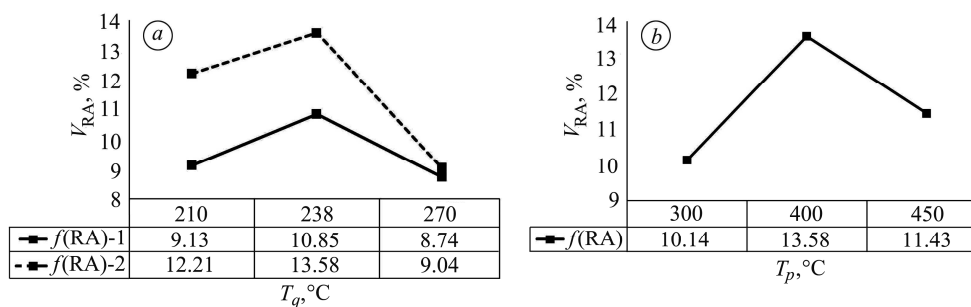


Fig. 6. Volume fraction of retained austenite for specimen quenched to 210, 238 and 270°C, partitioned at the same temperatures (–1); partitioned at 400°C (–2) (a) quenched to 238°C, partitioned at 300; 400 and 450°C (b).

CONCLUSION

An overview of the phase morphology during the application of one and two-step Q&P process for 37MnSi5 steel is presented. The most important observations are summarized as follows: a combination of carbon-enriched retained austenite with two types of morphological structures including film-like and island-like, and martensite with lath-type morphology as matrix were observed in all conditions in this study. Cementite-carbide precipitations within the martensite laths were also characterized in a sample quenched at 238°C and partitioned at 450°C for 100 s, and the dominant shape was quasispherical; an optimum quenching temperature in Q&P process ensures maximum carbon content for austenite that minimizes its M_s temperature, and so maximizes its thermal stability. The optimum quenching temperature of 238°C in this study could reduce the M_s temperature of austenite to -101.28°C and -60.93°C in one-step and two-step Q&P, respectively. With increase in a quench temperature from 210 to 270°C, the volume fraction of retained austenite first increased and arrived at a maximum at optimum quenching temperature (238°C), and then decreased. The volume fraction of retained austenite increased from 10.14 to 11.43% with increase in partitioning temperature from 300 to 450°C.

РЕЗЮМЕ. За останні два десятиліття спостерігають значну тенденцію до розвитку нових сталей третього покоління, які використовують в автомобільній промисловості. Шпеер запропонував нову термообробку – гартування/фрагментування (поділення), яка є новою стратегією виробництва сталей, які поєднують високу міцність та значну довговічність. Досліджено вплив температури гартування/фрагментування на морфологію та мікроструктуру сталі 37MnSi5. Для цього обрали такі температури старіння: 210; 238 та 270°C. Після термообробки визначали та порівнювали мікроструктурні характеристики з використанням сканівного електронного та емісійного мікроскопів.

РЕЗЮМЕ. За последние два десятилетия наблюдается значительная тенденция к развитию новых сталей третьего поколения, которые используют в автомобильной промышленности. Шпеер предложил новую термообработку – закалка/фрагментирование (разделение), которая является новой стратегией производства сталей, сочетающих высокую прочность и значительную долговечность. Исследовано влияние температуры закалки/фрагментирования на морфологию и микроструктуру стали 37MnSi5. Для этого выбрали такие температуры старения 210; 238 и 270°C. После термообработки определяли и сравнивали микроструктурные характеристики с использованием сканирующего электронного и эмиссионного микроскопов.

1. *Design of cold rolled and continuous annealed carbide-free bainitic steels for automotive application* / F. G. Caballero, S. Allain, J. Cornide, J. D. Puerta Velásquez, C. Garcia-Mateo, and M. K. Miller // *Mater. Des.* – 2013. – **49**. – 667 p.
2. *Strategies for third-generation advanced high-strength steel development* / E. De Moor, P. J. Gibbs, J. G. Speer, and D. K. Matlock // *AIST Trans.* – 2010. – **7**. – 133 p.

3. *Bhadেশia H. K. D. H.* The bainite transformation: unresolved issues // *Mater. Sci. Eng. A.* – 1999. – **273–275**. – P. 58.
4. Carbon partitioning into austenite after martensite transformation / J. G. Speer, D. K. Matlock, B. C. Cooman, and J. G. Schroch // *Acta Mater.* – 2003. – **51**. – 2611 p.
5. *Matlock D. K., Brautigam V. E., and Speer J. G.* Application of the quenching and partitioning (Q&P) process to a medium-carbon, high Si microalloyed bar steel // *Mater. Sci. Forum.* – 2003. – **426–432**. – 1089 p.
6. *Tamura I.* Deformation-induced martensitic transformation and transformation-induced plasticity in steels // *Met. Sci.* – 1982. – **16**. – 245 p.
7. *Matsumura O., Sakuma Y., and Takechi H.* Retained austenite in 0.4C–Si–1.2Mn steel sheet intercritically heated and austempered // *ISIJ Int.* – 1992. – **32**. – 1014 p.
8. *Austenite formation and decomposition* / J. G. Speer, A. M. Streicher, D. K. Matlock, F. C. Rizzo, and G. Krauss / Eds.: E. B. Damm, M. Merwin. – Warrendale, PA: TMS/ISS. – 2003. – P. 505.
9. *New low carbon Q&P steels containing film-like intercritical ferrite* / M. J. Santofimia, T. Nguyen-Minh, L. Zhao, R. Petrov, I. Sabirov, and J. Sietsma // *Mater. Sci. Eng. A.* – 2010. – **527**. – 6429 p.
10. *The “Quenching and Partitioning” Process: Background and Recent Progress* / J. G. Speer, F. C. Rizzo, D. K. Matlock, and D. V. Edmonds // *Mater. Res.* – 2005. – **8**. – 417 p.
11. *Microstructural development during the quenching and partitioning process in a newly designed low-carbon steel* / M. J. Santofimia, L. Zhao, R. Petrov, C. Kwakernaak, W. G. Sloof, and J. Sietsma // *Acta Mater.* – 2011. – **59**. – 6059 p.
12. *Toji Y., Miyamoto G., and Raabe D.* Carbon partitioning during quenching and partitioning heat treatment accompanied by carbide precipitation // *Acta Mater.* – 2015. – **86**. – 137 p.
13. *Characterization of the microstructure obtained by the quenching and partitioning process in a low-carbon steel* / M. J. Santofimia, L. Zhao, R. Petrov, and J. Sietsma // *Mater. Charact.* – 2008. – **59**. – 1758 p.
14. *Bainitic transformation during the two-step quenching and partitioning process in a medium carbon steel containing silicon* / H. Y. Li, X. W. Lu, X. C. Wu, Y. A. Min, and X. J. Jin // *Mater. Sci. Eng. A.* – 2010. – **527**. – 6255 p.
15. *Phase transformation and mechanical properties of si-free CMnAl transformation-induced plasticity-aided steel* / J. Mahieu, J. Maki, B.C. De Cooman, and S. Claessens // *Metall. Mater. Trans. A.* – 2002. – **33**. – 2573 p.
16. *Cullity B. D. and Stock S. R.* Elements of X-ray Diffraction. 3rd ed. – New York: Prentice Hall, 2001.
17. *Cullity B. B.* Elements of X-Ray Diffraction. 2nd ed. – Addison-Wesley Publishing Co., Inc., 1978.
18. *Effect of retained austenite stabilized via quench and partitioning on the strain hardening of martensitic steels* / E. De Moor, S. Lacroix, A. J. Clarke, J. Penning, and J. G. Speer // *Metall. Mater. Trans. A.* – 2008. – **39**. – 2586 p.
19. *Wang X.D., Guo Z. H., and Rong Y. H.* Mechanism exploration of an ultrahigh strength steel by quenching–partitioning–tempering process // *Mater. Sci. Eng. A.* – 2011. – **529**. – 35 p.
20. *Wang L. and Speer J. G.* Quenching and partitioning steel heat treatment // *Metallogr. Microstruct. Anal.* – 2013. – **2**. – 268 p.
21. *Fonstein N.* Advanced high strength sheet steels physical metallurgy // 1st ed., Design, Proc. and Propert. – 2015. – **XXII**. – 396 p.
22. *Quenching and partitioning martensite—A novel steel heat treatment* / D. V. Edmonds, K. He, F. C. Rizzo, B. C. De Cooman, D. K. Matlock, and J. G. Speer // *Mater. Sci. Eng. A.* – 2006. – **438–440**. – 25 p.
23. *Enhancement of the mechanical properties of a Nb-microalloyed advanced high-strength steel treated by quenching–partitioning–tempering process* / N. Zhong, X. D. Wang, L. Wang, and Y. H. Rong // *Mater. Sci. Eng. A.* – 2009. – **506**. – 111 p.

Received 12.04.2016